# Uncertainty and Irreproducibility of Triboelectricity Based on Interface Mechanochemistry

Giulio Fatti, Hyunseung Kim, Changwan Sohn, Minah Park, Yeong-won Lim, Zhuohan Li, Kwi-Il Park, Izabela Szlufarska, Hyunseok Ko, Chang Kyu Jeong, and Sung Beom Cho

Phys. Rev. Lett. **131**, 166201 — Published 19 October 2023

DOI: 10.1103/PhysRevLett.131.166201

# Uncertainty and irreproducibility of triboelectricity based on interface mechanochemistry

Giulio Fatti, Hyunseung Kim, Changwan Sohn, Minah Park, Yeong-won Lim, Zhuohan Li, Kwi-Il Park, Izabela Szlufarska, Hyunseok Ko, Chang Kyu Jeong*, Sung Beom Cho*

*** Corresponding authors**

**Sung Beom Cho** – Department of Materials Science and Engineering, Ajou University, Suwon, Gyeonggi-do, 16499, Republic of Korea; Department of Energy Systems Research, Ajou University, Suwon, Gyeonggi-do, 16499, Republic of Korea Email: csb@ajou.ac.kr

**Chang Kyu Jeong** - Division of Advanced Materials Engineering, Jeonbuk National University, Jeonju, Jeonbuk 54896, Republic of Korea; Department of Energy Storage/Conversion Engineering of Graduate School & Hydrogen and Fuel Cell Research Center, Jeonbuk National University, Jeonju, Jeonbuk 54896, Republic of Korea; Department of JBNU-KIST Industry-Academia Convergence Research, Jeonju, Jeonbuk 54896, Republic of Korea; Email: ckyu@jbnu.ac.kr

**Authors**

**Giulio Fatti –** Materials Digitalization Center, Korea Institute of Ceramic Engineering and Technology (KICET), Jinju, Gyeongsangnam-do, 52851, Republic of Korea

**Hyunseung Kim –** Division of Advanced Materials Engineering, Jeonbuk National University, Jeonju, Jeonbuk 54896, Republic of Korea; Department of Energy Storage/Conversion Engineering of Graduate School & Hydrogen and Fuel Cell Research Center, Jeonbuk National University, Jeonju, Jeonbuk 54896, Republic of Korea

**Changwan Sohn –** Division of Advanced Materials Engineering, Jeonbuk National University, Jeonju, Jeonbuk 54896, Republic of Korea; Department of Energy Storage/Conversion Engineering of Graduate School & Hydrogen and Fuel Cell Research Center, Jeonbuk National University, Jeonju, Jeonbuk 54896, Republic of Korea

**Minah Park –** Division of Advanced Materials Engineering, Jeonbuk National University, Jeonju, Jeonbuk 54896, Republic of Korea

**Yeong-won Lim –** Division of Advanced Materials Engineering, Jeonbuk National University, Jeonju, Jeonbuk 54896, Republic of Korea; Department of Energy Storage/Conversion Engineering of Graduate School & Hydrogen and Fuel Cell Research Center, Jeonbuk National University, Jeonju, Jeonbuk 54896, Republic of Korea

**Zhuohan Li** – Materials Science Division, Lawrence Berkeley National Laboratory, Berkeley, California 94720, United States of America

**Kwi-Il Park** – School of Materials Science and Engineering, Kyungpook National University, Daegu 41566, Republic of Korea

**Izabela Szlufarska** – Department of Materials Science and Engineering, University of Wisconsin-Madison, Madison, Wisconsin 53706-1595, United States of America

**Hyunseok Ko** - Materials Digitalization Center, Korea Institute of Ceramic Engineering and Technology (KICET), Jinju, Gyeongsangnam-do, 52851, Republic of Korea

**Abstract**

Triboelectrification (TE) mechanism is still not understood, despite centuries of investigations. Here, we propose a model showing that mechanochemistry is key to elucidate TE fundamental properties. Studying contact between gold and silicate glasses, we observe that the experimental triboelectric output is subject to large variations and polarity inversions. First principles analysis shows that electronic transfer is activated by mechanochemistry and the tribopolarity is determined by the termination exposed to contact, depending on the material composition, which can result in different charging at the macroscale. The electron transfer mechanism is driven by the interface barrier dynamics, regulated by mechanical forces. The model provides a unified framework to explain several experimental observations, including the systematic variations in the triboelectric output and the mixed positive-negative, "mosaic" charging patterns, and paves the way to the theoretical prediction of the triboelectric properties.

Triboelectrification (TE), the transfer of electrostatic charge between two materials in contact, is one of the longest studied physical problems. Despite being investigated since the 18$^{th}$ century [1, 2], very little conclusive understanding has been achieved on its underlying mechanism. For a long time, scientists believed that materials had an inherent tendency to charge more or less positively or negatively, and they devised the so-called triboelectric series to order materials according to their triboelectric charging [3-5]. However, several experimental observations conflict with the very idea of such ordering. Triboelectric series have proved uncertain and hard to reproduce [6]. Distinct samples of the same materials can change position on the triboelectric series, and triboelectric charging can change even on the same sample after consecutive experiments [5-10]. For instance, glasses and silicates are a major example of this irreproducibility, as they systematically show different charging in different experiments [4, 5, 11-14].

The reasons for this systematic irreproducibility have not been fully understood to date. In general, different charge carriers may govern the physics of TE, electrons [15-18], ions [19-21], and tiny fragments of material transferred in the contact [22-24]. Theoretical models have mostly focused on electron transfer, especially after recent experimental findings suggested that solid-solid TE is mainly caused by electrons [16, 17]. For example, the surface state model [25, 26], the effective work function model [27-29], and the interface potential barrier model [30] have been proposed to explain electron-driven TE. However, these models fail to reproduce the experimental observations. The more recent backflow-stuck charges (BSC) model proposed a more successful explanation [31], establishing a positive correlation between electron-driven triboelectric charging and the electrostatic potential barrier existing at the contact interface. A schematic defining the electrostatic barrier is shown in the Supplemental Material (SM), Note S1 [32]. According to the model, electron transfer is caused by mechanical forces upon contact, but some charges flow back to their original material through tunneling. Hence, only electrons remaining stuck after transfer contribute to TE. A higher electrostatic barrier thus prevents larger electron backflow and results in a higher TE. The BSC model has been able to capture some features of metal-dielectric TE, successfully describing the triboelectric series of tribopositive oxides.

However, even the most refined models based only on electron transfer cannot grasp the full complexity of the experimental measurements. First, in the tribology community it is universally accepted that mechanochemical reactions are ubiquitous in frictional contact, causing bond ruptures and ionic transfer [33-39]. Second, Atomic Force Microscopy (AFM) measurements have showed that nanoscale charging is always found in a mosaic of both positive and negative charged regions. Therefore, the net macroscopic charge is given by the balance between these mixed island of positive and negative charges [40-41]. These measurements have been reproduced several times [42-44], showing that this feature is universal and might be inherently related to ion transfer [22], whose mechanism has not been described yet.

In this work, combining experimental measurements and first principles calculations, we demonstrate that mechanochemistry and ion transfer are indeed key to trigger electron-driven TE. We analyzed a selected set of gold-silicates pairs, chosen for their especially unclear triboelectric behavior, and confirmed the inherent irreproducibility of the measurements, applying a statistical approach. To elucidate the underlying mechanism, we employed first principles calculations to devise the first theoretical mechanochemistry-based model of TE, generalizing the BSC model to include ionic transfer. The model shows that i) mechanochemistry can be crucial to prompt electron-driven TE, and that ii) tribopolarity is determined by the chemical properties of the surface terminations exposed by mechanochemistry, implying that only certain materials can switch polarity depending on their surface terminations chemical composition. Additionally, we tested our model on $TiO_2$, corroborating our results. Importantly, the model does not involve ions as charge carriers, but highlights how mechanochemical ion transfer can enable electron transfer. Hence, the model can be coherently combined with other recent models involving flexoelectricity and thermoelectricity [45-48]. Our findings explain a broad range of experimental observations, from the mosaic charge patterns to the irreproducible triboelectric series, including them in a unified theoretical framework.

Figure 1 shows our triboelectric measurements for the selected materials, namely quartz, fused silica, and borosilicate glass. The choice of these materials allows us to evaluate the contribution to TE played by chemical composition and crystallinity. Figure 1a schematically represents the triboelectric generator (TEG) employed for the measurements. TEGs can be designed in different operation modes that can collect tribocharges either by sliding or by vertical contact-separation (CS) motion [49]. We employed a CS configuration, schematically depicted in Figure 1a, to exclude complications arising from sliding motion, such as shear effects, for a better comparison with theoretical calculations. Contact with gold, chemically inert and triboelectrically neutral, guarantees a reliable evaluation of the triboelectric output. Further details are provided in the Methods 1 section of the SM.

According to previous reports [4, 5, 11-14], while fused and quartz silica occupy well-defined positions on the triboelectric series, borosilicate glass can switch polarity. Figure 1b shows a qualitative comparison between previously reported series. Our measurement distributions show that the actual triboelectric signal can significantly vary at every measurement, spanning a wide range of voltages and currents, respectively displayed in the violin plots in Figure 1c and d. For all three types of material, the distributions have long tails deviating from the bulk of the distribution, which demonstrates a wide uncertainty of the results. However, both fused silica and quartz reveal a steadily negative triboelectric charging and a similar distribution, while borosilicate shows a bimodal distribution, with two distinct peaks with opposite polarities. A complete list of references is in the SM, Note S2 [32]. Since the measurement distributions can be multimodal, like for borosilicate, the triboelectric series cannot be defined using the distribution average. This would fail to capture the triboelectric behavior, as it would predict an almost neutral output, instead of a triboelectric charge fluctuating between negative and positive. This is highlighted by the white dots representing the average of the distributions in Figure 1b and c.

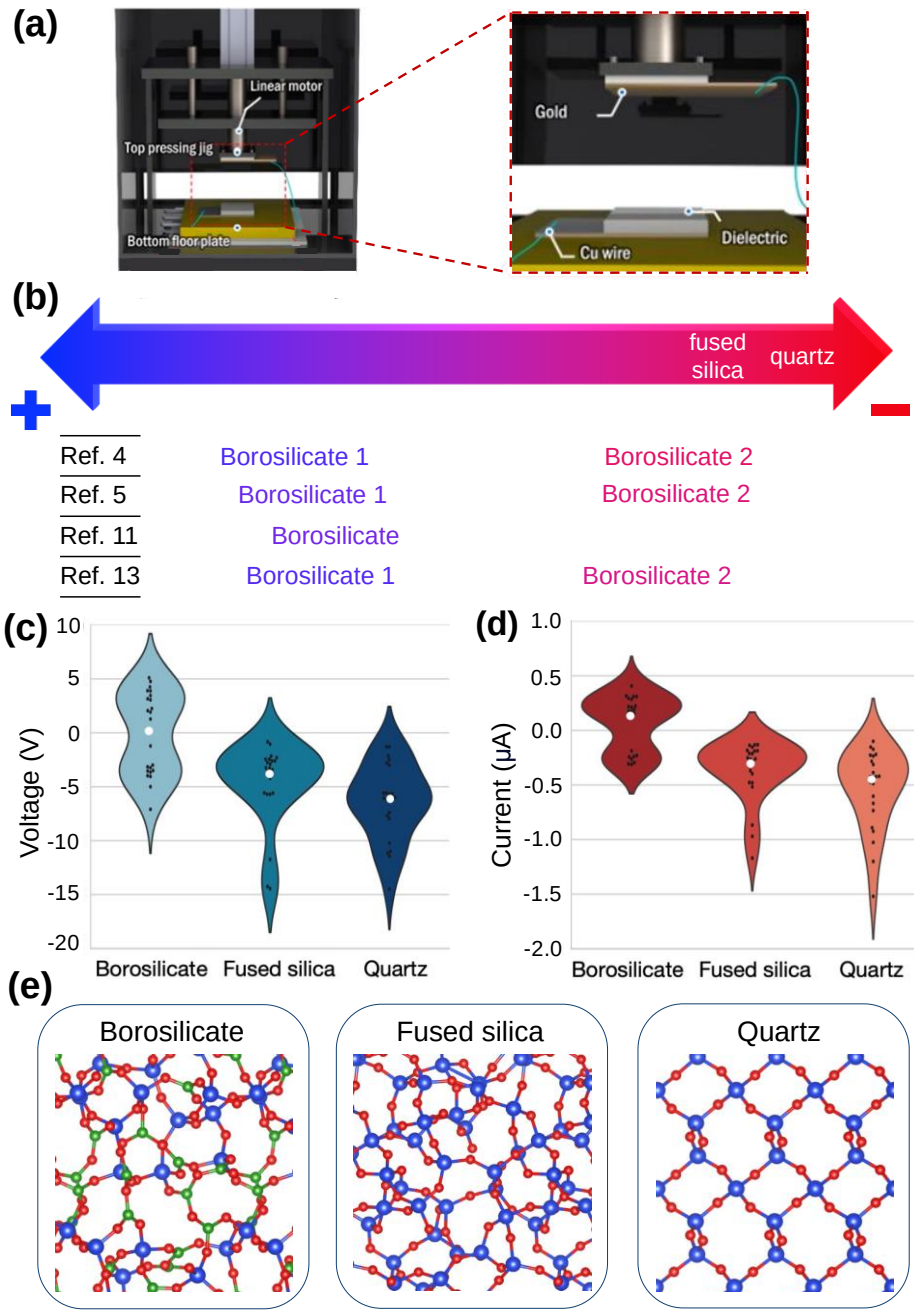


**Figure 1**: Triboelectrification experimental measurements of silica and borosilicate glass. (a) Schematics of the experimental apparatus for the vertical CS mode. (b) Qualitative triboelectric series extracted from references [4, 5, 11, 13]. (c), (d) Violin plots showing, respectively, the highly variable distribution of the measured voltages and currents. e) Snapshots of the borosilicate, fused silica and quartz structures as employed for the DFT calculations.

To understand the systematic uncertainty observed in the measurements, we investigated nanoscale contact by means of first-principles calculations. The employed structures are shown in

Figure1e and described accurately in the SM, Methods 3. First, we tested the BSC model, investigating the triboelectric behavior of the hydroxylated surfaces of the selected materials [50-52], involving only electron transfer [32]. Analyzing the partial charges by means of Bader analysis, we found a negligible triboelectric charging of $10^{-2}\ e$ and, coherently with the BSC model [31], a very low barrier at the gold/silicate interface. However, as this clearly contradicts the experimental measurements, electron transfer alone cannot explain TE, meaning that transfer of chemical species must be involved.

Therefore, we modeled silicate-gold contact under pressure to study the activation of hydrogen transfer by mechanical forces and to evaluate the effect on TE of the newly formed dangling bond. We applied a methodology first introduced to describe mechanochemical reactions from first principles [53]. In this method, the effect of pressure on chemistry is investigated by applying a quasi-static indentation of the silicates against gold. As shown in Figure 2a, we started from a fixed interface separation and relaxed the configuration before (initial configuration) and after (final configuration) ionic transfer. Using the calculated energies, we computed the reaction energy as $E_r = E_{final} - E_{initial}$. After relaxation we moved the silicate closer to the gold, relaxed again both the initial and the final configuration, re-computed the reaction energy, and iterated the process. More details on the procedure can be found in the SM, Note S5 [32]. Figures 2b and c show the reaction energy $E_r$ against the applied pressure for the hydrogen transfer from fused silica and quartz, respectively. The reaction becomes energetically favorable at very high pressures, in the order of the GPa, four order of magnitude larger than the nominal experimental pressure of $10^5$ Pa. However, it is known that nominally flat surfaces are comprised of multiple nano-asperities [54] and the local pressure on single asperities can be up to $10^5$ times higher than the macroscopic pressure applied experimentally, as shown in the SM, Figure S6 [32, 55-60]. The calculated pressure range is indeed consistent with previous measurements of single asperity contact [61]. In a real-life situation, flash temperatures and kinetic effects should contribute to further reducing the pressure needed to activate the mechanochemical reaction [62]. It should be noted that gold deforms

plastically, which is in agreement with previous reports where it has been observed even to a very large extent [63].

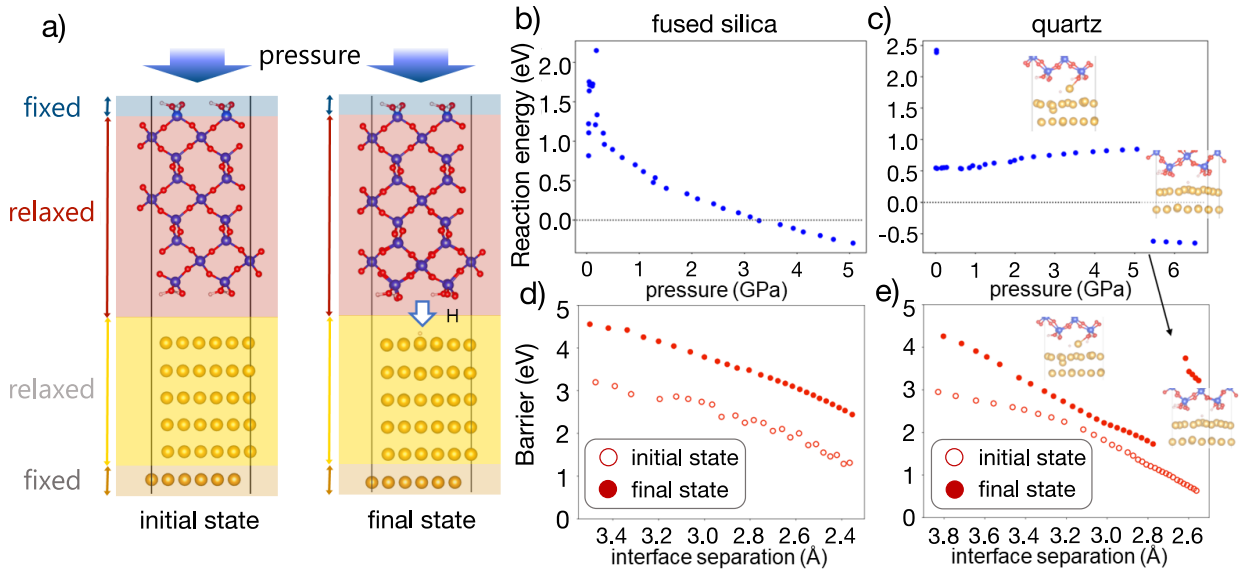


**Figure 2**: Effect of indentation on reaction energy and electrostatic barrier. a) Silica on gold indentation is modeled ab-initio simulating the initial (before mechanochemistry) and the final state (after) at a fixed interface distance, and then progressively reducing this distance to increase the pressure quasi-statically. b), d) Reaction energy at every indentation step, respectively for fused silica and quartz. c), e) Interface barrier before (unfilled circles) and after (filled circles) hydrogen transfer, respectively for fused silica and quartz.

Figures 2d and e show the evolution of the interface barrier as the indentation proceeds, before (unfilled circles) and after (filled circles) hydrogen transfer. Two major points emerge from these results. First, the barrier rises significantly after the mechanochemical reaction. This immediately points out to an increase in the triboelectric charging, according to the BSC model. Electronic transfer is indeed confirmed by calculations performed at the equilibrium. Note S7 in the SM show that different terminations exposed by mechanochemical reactions acquire a large charge, demonstrating that TE is enabled by mechanochemistry . This charge is fully electronic, with no ionic contribution, as shown in the SM, Note S8 [32]. Moreover, we find that the calculated electrostatic barrier and triboelectric charging are proportional, further corroborating the BSC model. Second, as silica and gold are pressed against each

other, the interfacial barrier reduces by as much as 50%. This barrier drop is significant because it facilitates electron transfer, as we have shown with a numerical simulation of the tunneling probability across the quantum barrier in the SM, Note S9. Experimentally, kinetic effects due to the non-equilibrium nature of contact, not present in the simulations, are likely to further contribute to the transfer [64]. Based on this consideration, we propose a mechanism to include mechanochemistry in the description of the microscopic TE process.

Figure 3 shows the scheme of our proposed model. We conceptually schematize the contact in three stages: approach, full contact, and separation. In the approaching stage (Figure 3a) the silicate gets closer to gold under the effect of external mechanical stresses. Initially, pressure is low, and no chemical reaction occurs. Since the barrier is low, any transferred charge is free to flow back to the more stable state on its original material. This stage corresponds to the unfilled dots in Figure 2d and e. As indentation proceeds, mechanical stresses activate mechanochemical reactions. This generates dangling bonds on the silicate surface which allow electronic transfer, resulting in a sudden barrier hike (the filled dots in Figure 2d and e), in agreement with the BSC model. Under increasing pressure, interface separation continues to narrow, lowering again the barrier and enabling additional charge transfer – the forward flow. This process shows that TE is indeed activated by mechanical stresses, an assumption of the BSC model that is demonstrated here.

At full contact stage (Figure 3b), triboelectric charging reaches its maximum value. First, the Fermi levels of gold and the silicate in contact are aligned, implying that the highest-occupied states in gold are energetically unfavorable with respect to defect states in the silicate, inducing a flow of electrons toward the more stable states.

During separation (Figure 3c) the excess charges captured by the silicate start to experience a drive to flow back to their original state due to the relief of pressure and the inversion of the kinetic motion. As pressure is relieved, electron backflow is activated by tunneling or lattice vibrations [31]. Backflow is stronger when the barrier is still low but, with increasing separation, the barrier progressively

raises and the backflow slows down until it eventually stops, as shown in the last step, Figure 3c. The height of the barrier governs how quickly the backflow completely stops and determines the final quantity of stuck charges. The mechanism here proposed improves and generalizes the BSC model to a much wider class of situations, describing the effect of mechanochemistry on TE in metal-dielectric contact.

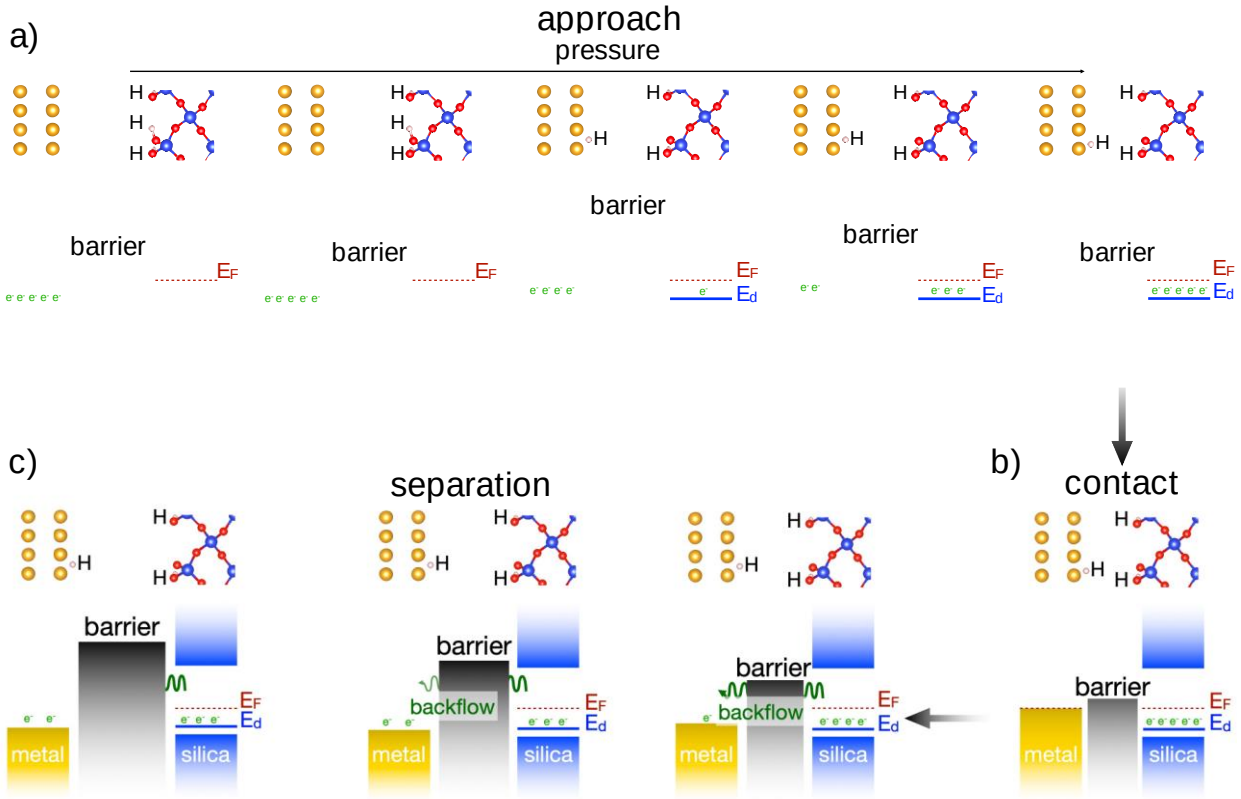


**Figure 3**: Mechanism of triboelectrification due to mechanochemical ion transfer. a) In the approaching stage initially triboelectrification is prevented by the absence of dangling bonds. As the pressure increases, mechanochemical ion transfer is activated and charge transfer begins (forward flow). The increasing pressure lowers the interface barrier and favors a larger charge transfer. b) At full contact the maximum amount of charge is transferred. c) During separation a fraction of the transferred charges flow back to gold, tunneling the barrier (backflow), until it becomes too high to be tunneled.

Once explained the mechanochemical process, we investigated the influence of different terminations on tribopolarity. We considered two possible mechanochemical reactions leading to ionic transfer and to the exposure of dangling bonds to contact:

$$\text{Au} + \text{silicate-OH} \rightarrow \text{Au-H} + \text{silicate-O-} \quad (1)$$

$$\text{Au} + \text{silicate-OH} \rightarrow \text{Au-OH} + \text{silicate-} \quad (2)$$

Reaction (1) breaks the O−H bond and exposes the oxygen anion to contact. Reaction (2) severs the bond between oxygen and the cation, leaving a dangling bond on silicon in fused silica and quartz, and on silicon or boron in borosilicate. Figure 4a shows the possible terminations for each considered material and their calculated triboelectric charging at the equilibrium interface distance. Borosilicate has four possible terminations, Si−, B−, SiO− and BO−, while fused silica and quartz have only Si− and SiO−. In both fused silica and quartz the calculated triboelectric charging is negative for each termination, consistently with previous studies performed by means of high-accuracy first-principles investigations [65-67], supported by experimental evidence [68-69]. These reports have demonstrated that both SiO− and Si− surface defects act as deep electron traps, consistent with our finding that both terminations contribute to negative TE. Borosilicate can instead switch tribopolarity depending on the termination. As shown in Figure 4a, cationic Si− and B− acquire positive tribocharge, while the anionic SiO− and BO− charge negatively.

Figure 4b shows a schematic of the mechanism leading to different TE observed between pure silica and borosilicate. This can be related to their different chemical composition. In pure silica, both anionic (O−) and cationic (Si−) terminations contribute to negative triboelectric charging, while in borosilicate they switch polarity. This suggests an explanation for the high variability observed in the experiments. Experimentally, the macroscopic TE output will be determined by the charge balance induced by the occurrence of multiple mechanochemical reactions. Several anionic and cationic terminations will be exposed, each contributing to triboelectric charging. The effect of plastic deformation will then promote the local convergence of positive or negative terminations, forming separate positive and negative areas [40, 70]. This arrangement breaks the equiprobability between asperities of opposite polarities, leading to a non-neutral macroscopic charging, depending on the details and history of contact

and on the environmental conditions (SM, Note S10). Thus, borosilicate charging can oscillate between tribopositivity and tribonegativity, depending on whether positive or negative areas come to be dominant at the interface. On the other hand, because silica terminations are always tribonegative, its macroscopic TE output will always be negative, even though it can change in magnitude with the number of actual mechanochemical events. In this case, the different number of mechanochemical events occurring at every measurement can also explain the distribution of the silica triboelectric output, as more reactions induce a larger charging and *vice versa*. Finally, borosilicate samples often contain concentrations of sodium oxide ($Na_2O$) that can contribute to TE, as shown in the SM, Note S11 [71]. The mechanism is corroborated by the results on the additional test material $TiO_2$, shown in Note S12.

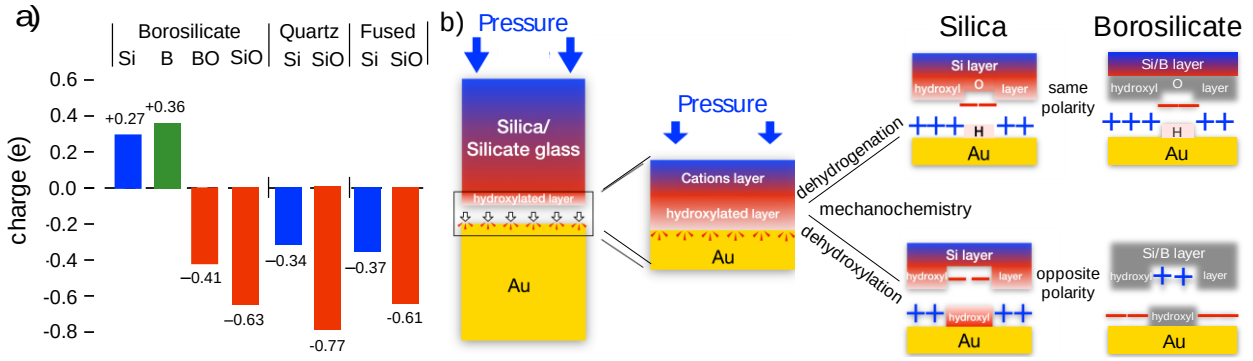


**Figure 4**: Tribopolarity connected to different terminations. a) Triboelectrification of the possible terminations respectively for borosilicate, quartz and fused silica, expressed in elementary charge units *e*. b) Schematics of the tribopolarity mechanism. Mechanochemical bonds rupture prompt charge transfer on the exposed anions or cations. These charge negatively in pure silica, while borosilicate cations charge positively.

In conclusion, we have proposed a mechanochemical model for TE to explain the systematic uncertainty observed in the experimental measurements. By investigating the contact between selected silicates and gold as a notable case study, we have shown that electronic transfer is enabled by the mechanochemical reactions occurring at the nano-asperities in contact. We have further generalized the BSC model, showing that the dynamics of electronic transfer is regulated by the variation of the interface barrier in the contact-separation motion. Through the model we have demonstrated that the tribopolarity of a material is

determined by what terminations are exposed to contact. For example, cationic terminations are tribonegative in pure silica but tribopositive in borosilicate. The macroscopic triboelectric output will be then governed by the surface balance between the positive and negative terminations. These findings explain several experimental observations, from the uncertain triboelectric output to the mosaic charging patterns, unifying them in a comprehensive theoretical framework. Moreover, our model is complementary to other models that have recently tried to explain TE based on the high stresses at the nanoasperity contact, highlighting the role of flexoelectricity or thermoelectricity [44-47]. Relating TE to the chemical properties of the species composing a material, we pave the way for the theoretical prediction of TE.

We gratefully acknowledge the support from the National Research Foundation of Korea funded by the Korean government (2022R1A2C4002037, 2022R1A4A3032923, RS-2023-00209910, and 2022-R1F1A1093060). The computations were carried out using resources from Korea Supercomputing Centers (KSC-2022-CRE-0042). ZL and IS gratefully acknowledge support from the US National Science Foundation grant #1951314.

## References

[1] P. Shaw. (1917). «Experiments on tribo-electricity. I.—The tribo-electric series». *Nature*, Proceedings of the Royal Society of London. Series A, Containing Papers of a Mathematical and Physical Character, 94(656), 16-33.

[2] D. J. Lacks and T. Shinbrot. (2019). «Long-standing and unresolved issues in triboelectric charging». *Nature Reviews Chemistry,* 3(8), 465-476.

[3] H. Zou, Y. Zhang, L. Guo, P. Wang, X. He, G. Dai, H. Zheng, C. Chen, A. C. Wang, C. Xu and Z. L. Wang. (2019). «Quantifying the triboelectric series». *Nature Communications,* 10(1), 1-9.

[4] A. Diaz and R. Felix-Navarro. (2004) «A semi-quantitative tribo-electric series for polymeric materials: the influence of chemical structure and properties». *Journal of Electrostatics,* 62(4), 277-290.

[5] D. M. Gooding and G. K. Kaufman. (2011) «Tribocharging and the triboelectric series». *Encyclopedia of Inorganic and Bioinorganic Chemistry,* 1-14.

[6] D. J. Lacks. (2012). «The Unpredictability of Electrostatic Charging». *Angewandte Chemie International Edition,* 51(28), 6822-6823.

[7] F. Shonebarger and H. H. Blau. (1966). «Study of Glass Surfaces by Generation of Electrostatic Charges,» *Journal of the American Ceramic Society*. 49(9), 492-497.

[8] J. F. Kok and N. O. Renno. (2008). «Electrostatics in Wind-Blown Sand,» *Physical Review Letters, 100*(1), 014501.

[9] G. Castle. (1997). «Contact charging between insulators,» *Journal of Electrostatics, 40*, 13-20.

[10] J. Zhang, C. Su, F. J. M. Rogers, N. Darwish, M. L. Coote and S. Ciampi. (2020). «Irreproducibility in the triboelectric charging of insulators: evidence of a non-monotonic charge versus contact time relationship». *Physical Chemistry Chemical Physics, 22*(20), 11671-11677.

[11] H. Zuo, L. Guo, H. Xue, Y. Zhang, X. Shen, X. Liu, P. Wang, X. He, G. Dai, P. Jiang, H. Zheng, B. Zhang, C. Xu and Z. L. Wang. (2020). «Quantifying and understanding the triboelectric series of inorganic non-metallic materials». *Nature communications, 11*(1), 1-7.

[12] D. Ferguson. (2010). «A basic triboelectric series for heavy minerals from inductive electrostatic separation behaviour». *Journal of the Southern African Institute of Mining and Metallurgy, 110*(2), 75-78.

[13] G. Freeman and N. March. (1999). «Triboelectricity and some associated phenomena». *Materials science and technology, 15*(12), 1454-1458.

[14] J. Henniker. (1962). «Triboelectricity in Polymers». *Nature, 196*(4853), 474.

[15] Z. L. Wang and A. C. Wang. (2019). «On the origin of contact-electrification». *Materials Today, 30*, 34-51.

[16] C. Xu, Y. Zi, A. C. Wang, H. Zou, Y. Dai, X. He, P. Wang, Y.-C. Wang, P. Feng, D. Li and Z. L. Wang. (2018). «On the Electron-Transfer Mechanism in the Contact-Electrification Effect». *Advanced Materials, 30*(15), 1706790.

[17] S. Lin, L. Xu, C. Xu, X. Chen, A. C. Wang, B. Zhang, P. Lin, Y. Yang, H. Zhao e Z. L. Wang. (2019). «Electron Transfer in Nanoscale Contact Electrification: Effect of Temperature in the Metal–Dielectric Case». *Advanced Materials, 31*(17), 1808197.

[18] S. Park, J. Park, Y.-g. Kim, S. Bae, T.-W. Kim, K.-I. Park, B. H. Hong, C. K. Jeong and S.-K. Lee. (2020). «Laser-directed synthesis of strain-induced crumpled MoS2 structure for enhanced triboelectrification toward haptic sensors». *Nano Energy, 78*, 105266.

[19] A. F. Diaz, D. Wollmann and D. Dreblow. (1991). «Contact electrification: ion transfer to metals and polymers». *Chemistry of Materials, 3*(6), 997-999.

[20] L. S. McCarty and G. M. Whitesides. (2008) «Electrostatic Charging Due to Separation of Ions at Interfaces: Contact Electrification of Ionic Electrets». *Angewandte Chemie International Edition, 47*(12), 2188-2207.

[21] L. S. McCarty, A. Winkleman and G. M. Whitesides. (2007). «Ionic Electrets: Electrostatic Charging of Surfaces by Transferring Mobile Ions upon Contact». *Journal of the American Chemical Society, 129*(13), 4075-4088.

[22] H. T. Baytekin, B. Baytekin, J. T. Incorvati and B. A. Grzybowski. (2012) «Material Transfer and Polarity Reversal in Contact Charging». *Angewandte Chemie International Edition, 51*(20), 4843-4847.

[23] A. Ciniero, G. Fatti, M. C. Righi, D. Dini and T. Reddyhoff. (2019) «A combined experimental and theoretical study on the mechanisms behind tribocharging phenomenon and the influence of triboemission». *Tribology Online, 14*(5), 2019.

[24] L. Lapčinskis, A. Linarts, K. Mālnieks, H. Kim, K. Rubenis, K. Pudzs, K. Smits, A. Kovaļovs, K. Kalniņš, A. Tamm, C. K. Jeong and A. Šutka. (2021). «Triboelectrification of nanocomposites using identical polymer matrixes with different concentrations of nanoparticle fillers». *Journal of Materials Chemistry A, 9*(14), 8984-8990.

[25] D. J. Lacks, N. Duff and S. K. Kumar. (2008) «Nonequilibrium Accumulation of Surface Species and Triboelectric Charging in Single Component Particulate Systems,» *Physical review letters, 100*(18), 188305.

[26] L. Ernst. (1976). «Optical spectroscopy of surface states on NaCl and KCl crystals and its relation to contact charging». *Solid State Communications, 19*(4), 515-521.

[27] F.-C. Chiu. (2014). «A Review on Conduction Mechanisms in Dielectric Films». *Advances in Materials Science and Engineering, 2014*, 578168.

[28] A. Franciosi and C. G. Van de Walle. (1996) «Heterojunction band offset engineering». *Surface Science Reports, 25*(1-4), 1-140.

[29] Z. Zhong and P. Hansmann. (2017) «Band Alignment and Charge Transfer in Complex Oxide Interfaces». *Physical Review X, 7*(1), 011023.

[30] J. Wu, X. Wang, H. W. Li, Feng, W. Yang and Y. Hu. (2018). «Insights into the mechanism of metal-polymer contact electrification for triboelectric nanogenerator via first-principles investigations». *Nano Energy, 48*, 607-616.

[31] H. Ko, Y.-w. Lim, S. Han, C. K. Jeong and S. B. Cho. (2021). «Triboelectrification: Backflow and Stuck

Charges Are Key». *ACS Energy Letters, 6*(8), 2792–2799.

[32] See Supplemental Material at *[url]* for more details, which includes Ref. [5, 11, 22, 31, 40, 51, 53, 59-60, 63, 70, 72-96]

[33] F. Galembeck, T. Burgo, L. Balestrin, R. Gouveia, C. Silva and A. Galembeck. (2014). «Friction, tribochemistry and triboelectricity: recent progress and perspectives». *RSC Advances, 4*(109), 64280-64298.

[34] A. L. Barnette, D. B. Asay, D. Kim, B. D. Guyer, H. Lim, M. J. Janik and S. H. Kim. (2009). «Experimental and Density Functional Theory Study of the Tribochemical Wear Behavior of SiO2 in Humid and Alcohol Vapor Environments». *Langmuir, 25*(22), 13052–13061.

[35] H. He, L. Qian, C. G. Pantano and S. H. Kim. (2015). «Effects of humidity and counter-surface on tribochemical wear of soda-lime-silica glass». *Wear,* i, 100-106.

[36] M. Wang, F. Duan and X. Mu. (2019). «Effect of Surface Silanol Groups on Friction and Wear between Amorphous Silica Surfaces». *Langmuir, 35*(16), 5463–5470.

[37] T. D. Jacobs and R. W. Carpick. (2013). «Nanoscale wear as a stress-assisted chemical reaction». *Nature Nanotechnology, 8*(2), 108-112.

[38] Y. Liu and I. Szlufarska. (2012). «Chemical Origins of Frictional Aging». *Physical Review Letters, 109*(18), 186102,.

[39] R. Carpick, R. Bernal, P. Chen, J. Schall, J. Harrison and Y. Jeng. (2018). «Influence of Chemical Bonding on the Variability of Diamond-Like Carbon Nanoscale Adhesion: An In-Situ TEM/Nanoindentation and Molecular Dynamics Study». *Microscopy and Microanalysis, 24*(S1), 1822-1823,.

[40] H. Baytekin, A. Patashinski, M. Branicki, B. Baytekin, S. Soh and B. Grzybowski. (2011). «The Mosaic of Surface Charge in Contact Electrification,» *Science, 333*(6040), 302-312.

[41] T. A. Burgo, T. R. Ducati, K. R. Francisco, K. J. Clinckspoor, F. Galembeck and S. E. Galembeck. (2012). «Triboelectricity: Macroscopic Charge Patterns Formed by Self-Arraying Ions on Polymer Surfaces». *Langmuir, 28*(19), 7407-7416.

[42] R. F. Gouveia, C. A. Costa and F. Galembeck. (2008). «Water Vapor Adsorption Effect on Silica Surface Electrostatic Patterning». *Journal of Physical Chemistry C, 112*(44), 17193–17199.

[43] T. R. Ducati, L. H. Simões and F. Galembeck. (2010). «Charge Partitioning at Gas−Solid Interfaces: Humidity Causes Electricity Buildup on Metals». *Langmuir, 26*(17), 13763–13766.

[44] K. S. Moreira, D. Lermen, Y. A. S. da Campo, L. O. Ferreira and T. A. Burgo. (2020). «Spontaneous

Mosaics of Charge Formed by Liquid Evaporation». *Advanced Materials Interfaces, 7*(18), 2000884.

[45] C. Mizzi, A. Lin and L. Marks. (2019). «Does Flexoelectricity Drive Triboelectricity? ». *Physical Review Letters, 123*(11), 116103.

[46] C. Mizzi and L. Marks. (2022). «When Flexoelectricity Drives Triboelectricity». *Nano Letters, 22*(10), 3939–3945.

[47] K. Olson, C. Mizzi and L. Marks. (2022). «Band Bending and Ratcheting Explain Triboelectricity in a Flexoelectric Contact Diode». *Nano Letters, 22*(10), 3914–3921.

[48] E. C. Shin, J. H. Ko, H. K. Lyeo and Y. H. Kim. (2022). «Derivation of a governing rule in triboelectric charging and series from thermoelectricity». *Physical Review Research, 4*(2), 023131.

[49] Z. L. Wang. (2013). «Triboelectric Nanogenerators as New Energy Technology for Self-Powered Systems and as Active Mechanical and Chemical Sensors». *ACS Nano, 7*(11), 9533-9557.

[50] F. Tielens, C. Gervais, J. F. Lambert, F. Mauri and D. Costa. (2008). «Ab Initio Study of the Hydroxylated Surface of Amorphous Silica: A Representative Model». *Chemistry of Materials,* vol. 20, n. 10, pp. 3336-3344.

[51] A. Rimola, D. Costa, M. Sodupe, J.-F. Lambert and P. Ugliengo. (2013). «Silica Surface Features and Their Role in the Adsorption of Biomolecules: Computational Modeling and Experiments». *Chemical reviews, 113*(6), 4216-4313.

[52] H. Jabraoui, T. Charpentier, S. Gin, J.-M. Delaye and R. Pollet. (2021). «Atomic Insights into the Events Governing the Borosilicate Glass−Water Interface». *The Journal of Physical Chemistry C,* 125(149), 7919-7931.

[53] Z. Li and I. Szlufarska. (2021). «Physical Origin of the Mechanochemical Coupling at Interfaces». *Physical Review Letters, 126*(7), 076001.

[54] F. P. Bowden and D. Tabor. (1951). «The Friction and Lubrication of Solids». *American Journal of Physics, 19*(7), 428-429.

[55] I. Singer and H. Pollock. (1991) Fundamentals of friction: macroscopic and microscopic processes, vol. 220, Braunlage, Harz: Springer Science & Business Media.

[56] L.-T. Li, X.-M. Liang, Y.-Z. Xing, D. Yan and G.-F. Wang. (2021) «Measurement of Real Contact». *Journal of Tribology, 143*(7), 071501.

[57] P. Piotrowski, R. Cannara, G. Gao, J. Urban, R. Carpick and J. Harrison. (2010). «Atomistic Factors Governing Adhesion between Diamond, Amorphous Carbon and Model Diamond Nanocomposite Surfaces». *Journal of adhesion science and technology, 24*(15-16), 2471-2498.

[58] F. P. Bowden and D. Tabor. (1939). «The area of contact between stationary and moving surfaces».

*Proceedings of the Royal Society of London. Series A. Mathematical and Physical Sciences, 169*(938), 391-413.

[59] T. D. Jacobs and A. Martini. (2017). «Measuring and understanding contact area at the nanoscale: a review». *Applied Mechanics Reviews, 69*(6), 060802, 2017.

[60] V. A. Yastrebov, G. Anciaux and J.-F. Molinari. (2015). «From infinitesimal to full contact between rough surfaces: Evolution of the contact area». *International Journal of Solids and Structures, 52*, 83-102.

[61] N. Gosvami, B. J. F. Mangolini, A. Konicek, D. Yablon and R. Carpick. (2015). «Mechanisms of antiwear tribofilm growth revealed in situ by single-asperity sliding contacts». *Science, 348*(6230), 102-106.

[62] M. Kalin. (2004). «Influence of flash temperatures on the tribological behaviour in low-speed sliding: a review». *Materials Science and Engineering: A, 374*(1-2), 390-397.

[63] L.-F. Wang, Y. Dong, M.-H. Hu, J. Tao, J. Li and Z.-D. Dai. (2022). «Evolution of surfaces and mechanisms of contact electrification between metals and polymers». *Chinese Physics B, 31*(6), 066202.

[64] X. Han, K. Asare-Yeboah, Z. He, C. Jiang and S. Bi. (2023). «Mosaic Charge Distribution-Based Sliding and Pressing Triboelectrification under Wavy Configuration». *Journal of Physical Chemistry Letters, 14*(10), 2509-2517.

[65] G. Livia, P. V. Susho, G. Pacchioni and A. L. Shluger. (2007) «Electron Trapping at Point Defects on Hydroxylated Silica Surfaces,» *Physical Review Letters, 99*(13), 136801.

[66] A.-M. El-Sayed, M. B. Watkins, V. V. Afanas'ev and A. L. Shluger. (2014) «Nature of intrinsic and extrinsic electron trapping in SiO2,» *Physical Review B, 89*(12), 125201.

[67] F. U. P. Musso, X. Solans-Monfort and M. Sodupe. (2010) «Periodic DFT Study of Radical Species on Crystalline Silica Surfaces,» *Journal of Physical Chemistry C, 114*(39), 16430-16438.

[68] G. Pacchioni, L. Skuja and D. L. Griscom. (2012). Defects in SiO2 and related dielectrics: science and technology., Springer Science & Business Media.

[69] E. Bussmann and C. Williams. (2006) «Single-electron tunneling force spectroscopy of an individual electronic state in a nonconducting surface,» *Applied physics letters, 88*(26), 263108.

[70] O. Verners, L. Lapčinskis, L. Ģermane, A. Kasikov, M. Timusk, K. Pudzs, A. V. Ellis, P. C. Sherrell and A. Šutka. (2022). «Smooth polymers charge negatively: Controlling contact electrification polarity in polymers,» *Nano Energy, 104*, 107914.

[71] M. S. Smedskjaer, J. C. Mauro, R. E. Youngman, C. L. Hogue, P. Marcel e Y. Yue. (2011). «Topological

Principles of Borosilicate Glass Chemistry». *Journal of Physical Chemistry B, 115*(44), 12930–12946.

[72] [First reference in the Supplemental Material not already in the paper] G. Kresse, and J. Furthmüller. (1996). «Efficiency of ab-initio total energy calculations for metals and semiconductors using a plane-wave basis set». *Computational Materials Science, 6*(1), 15-50.

[73] J. P. Perdew, K. Burke, and M. Ernzerhof. (1996). «Generalized Gradient Approximation Made Simple». *Physical Review Letters*, *77*(18), 3865.

[74] G. Kresse, and D. Joubert. (1999) «From ultrasoft pseudopotentials to the projector augmented-wave method». *Physical Review B*, *59*(3), 1758.

[75] P. E. Blöchl. (1994). «Projector augmented-wave method». *Physical Review B*, *50*(24), 17953.

[76] A. Jain, S. P. Ong, G. Hautier, W. Chen, W. D. Richards, S. Dacek , S. Cholia, D. Gunter, D. Skinner, G. Ceder, and K. A. Persson. (2013). «Commentary: The Materials Project: A materials genome approach to accelerating materials innovation». *APL Materials*, *1*(1), 011002.

[77] S. P. Ong, W. D. Richards, A. Jain, G. Hautier, M. Kocher, S. Cholia, D. Gunter, V. L. Chevrier, K. A. Persson, and G. Ceder. (2013). «Python Materials Genomics (pymatgen): A robust, open-source python library for materials analysis». *Computational Materials Science*, *68*, 314-319.

[78] A. Pedone, G. Malavasi, M. C. Menziani, U. Segre, and Cormack, A. N. (2008). «Molecular dynamics studies of stress− strain behavior of silica glass under a tensile load». *Chemistry of Materials*, *20*(13), 4356-4366.

[79] D. J. Evans, and B. L. Holian. (1985). «The nose–hoover thermostat». *The Journal of chemical physics*, *83*(8), 4069-4074.

[80] W. Tang, E. Sanville, and G. Henkelman. (2009). «A grid-based Bader analysis algorithm without lattice bias». *Journal of Physics: Condensed Matter*, *21*(8), 084204.

[81] E. Sanville, S. D. Kenny, R. Smith, and G. Henkelman. (2007). «Improved grid-based algorithm for Bader charge allocation». *Journal of computational chemistry*, *28*(5), 899-908.

[82] M. Yu, and D. R. Trinkle. (2011). «Accurate and efficient algorithm for Bader charge integration». *The Journal of chemical physics*, *134*(6).

[83] M. L. Hair. (1975). «Hydroxyl groups on silica surface». *Journal of Non-Crystalline Solids*, *19*, 299-309.

[84] A. S. D'Souza, and C. G. Pantano. (1999). «Mechanisms for silanol formation on amorphous silica fracture surfaces». *Journal of the American Ceramic Society*, *82*(5), 1289-1293.

[85] W. A. Adeagbo, N. L. Doltsinis, K. Klevakina, and J. Renner. (2008). «Transport processes at α-Quartz–water interfaces: insights from first-principles molecular dynamics

simulations». *ChemPhysChem: A European Journal of Chemical Physics and Physical Chemistry*, *9*(7), 994-1002.

[86] Á. Cimas, F. Tielens, M. Sulpizi, M. P. Gaigeot, and D. Costa. (2014). The amorphous silica–liquid water interface studied by ab initio molecular dynamics (AIMD): local organization in global disorder». *Journal of Physics: Condensed Matter*, *26*(24), 244106.

[87] A. Rimola, D. Costa, M. Sodupe, J. F. Lambert, and P. Ugliengo. (2013). «Silica surface features and their role in the adsorption of biomolecules: computational modeling and experiments». *Chemical reviews*, *113*(6), 4216-4313.

[88] L. T. Zhuravlev, and V. V. Potapov. (2006). «Density of silanol groups on the surface of silica precipitated from a hydrothermal solution». *Russian journal of physical chemistry*, *80*(7), 1119-1128.

[89] L. T. Zhuravlev. (2000). «The surface chemistry of amorphous silica. Zhuravlev model». *Colloids and Surfaces A: Physicochemical and Engineering Aspects*, *173*(1-3), 1-38.

[90] T. M. Mayer, J. E. Houston, G. E. Franklin, A. A. Erchak, and T. A. Michalske. (1999). «Electric field induced surface modification of Au. *Journal of applied physics*, *85*(12), 8170-8177.

[91] Multiphysics, C. O. M. S. O. L. (1998). «Introduction to COMSOL multiphysics®». *COMSOL Multiphysics, Burlington, MA, accessed Feb*, *9*(2018), 32.

[92] O. Verners, L. Lapčinskis, L. Ģermane, A. Kasikov, M. Timusk, K. Pudzs, A. V. Ellis, P. C. Sherrell, and A. Šutka, (2022). «Smooth polymers charge negatively: Controlling contact electrification polarity in polymers». *Nano Energy*, *104*, 107914.

[93] D. G. Jeong, Y. J. Ko, J. H. Kim, D. S. Kong, Y. C. Hu, D. W. Lee, S. H. Im, J. Lee, M. S. Kim, G.-H. Lee, C. W. Ahn, J. R. Ahn, M. Lee, J. Y. Park, and J. H. Jung. (2022). «On the origin of enhanced power output in ferroelectric polymer-based triboelectric nanogenerators: Role of dipole charge versus piezoelectric charge». *Nano Energy*, *103*, 107806.

[94] M. Rarivomanantsoa, P. Jund, and R. Jullien. (2004). «Sodium diffusion through amorphous silica surfaces: A molecular dynamics study». *The Journal of chemical physics*, *120*(10), 4915-4920.

[95] N. V. Tran, A. K. Tieu., H. Zhu, H. T. Ta, P. T. Sang, H. M. Le, and Ta, T. D. (2020). «Insights into the tribochemistry of sliding iron oxide surfaces lubricated by sodium silicate glasses: An ab initio molecular dynamics study». *Applied Surface Science*, *528*, 147008.

[96] [Last reference in the Supplemental Material not already in the paper] M. Ren, L. Deng, and J. Du. (2017). «Bulk, surface structures and properties of sodium borosilicate and boroaluminosilicate nuclear waste glasses from molecular dynamics simulations». *Journal of Non-Crystalline Solids*, *476*, 87-94.